Drell-Yan Production of W/Z at the LHC with Protons and Heavy Nuclei

D. Benjamin Clark Fred Olness

Southern Methodist University (Dallas,TX)

DPF 2015
Ann Arbor, MI

4 August 2015

nPDFs and Nuclear Corrections

Nuclear Modifications to PDFs

- Nuclear PDFs (nPDFs) can show significant modifications to free proton PDFs.

- DIS data suggest several types of corrections:
  - Shadowing
    $x < 0.05 - 0.1$
  - Anti-shadowing
    $0.1 \le x \le 0.3$
  - EMC effect
    $0.3 \le x \le 0.8$
  - Fermi motion
    $x > 0.8$

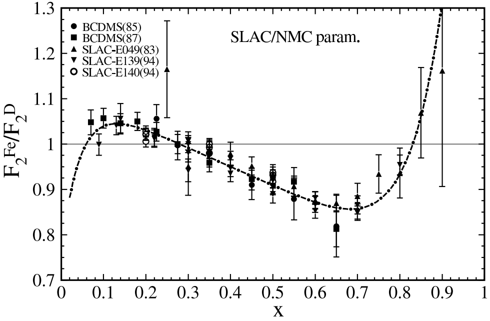

(Schienbein et. al. arXiv:0907.2357v2)

Nuclear Modifications

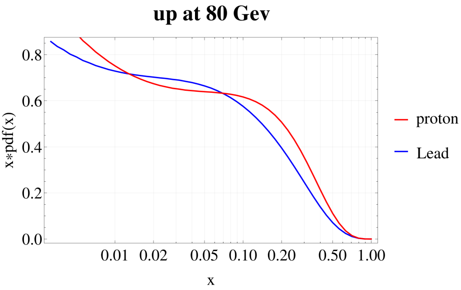

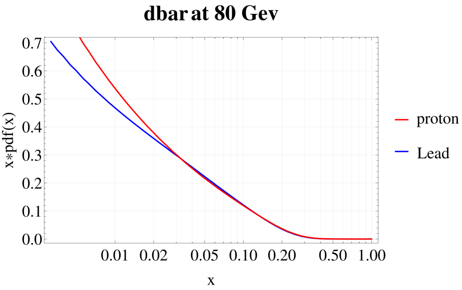

- The nuclear modifications are present in the PDFs, but appear in different regions of x than for the observables.
- We expect modifications to any hadronic observable involving heavy nuclei.

nCTEQ PDFs

- The nCTEQ proton PDFs are parameterized according to the following prescription;

$$
\begin{aligned}
x\, f_k(x, Q_0) &= c_0 x^{c_1}(1-x)^{c_2} e^{c_3 x}(1+e^{c_4} x)^{c_5} \\
k &= u_v, d_v, g, \bar{u}+\bar{d}, s, \bar{s}\,, \\
\bar{d}(x, Q_0)/\bar{u}(x, Q_0) &= c_0 x^{c_1}(1-x)^{c_2} + (1+c_3 x)(1-x)^{c_4}
\end{aligned}
$$

- The nuclear A-dependence is then applied to the coefficients in the parameterization.

$$c_k \to c_k(A) \equiv c_{k,0} + c_{k,1}\left(1 - A^{-c_{k,2}}\right), \quad k = \{1, \ldots, 5\}$$

(Schienbein et. al. arXiv:0907.2357v2)

EPS PDFs

- Another popular nPDF set is EPS09.

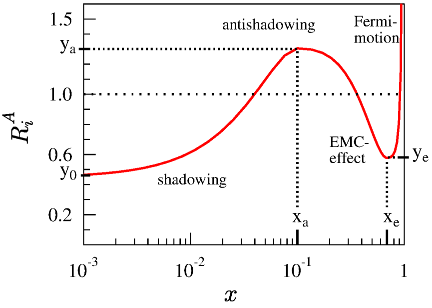

- In this analysis, an x-dependent nuclear correction is factorized from a fixed proton PDF.

$$f_i^A(x, Q) \equiv R_i^A(x, Q) f_i^{\mathrm{p}}(x, Q),$$

nCTEQ PDFs

- The nCTEQ group has produced a several sets of nuclear nPDFs at NLO for public distribution.

(Schienbein et. al. arXiv:0907.2357v2)

(Stavreva et. al. arXiv:1012.1178)

- The PDF for a general nucleus can be constructed as a linear combination of the PDFs using (approximate) isospin symmetry

$$f_i^{(A,Z)}(x,Q) = \frac{Z}{A}\, f_i^{p/A}(x,Q) + \frac{(A-Z)}{A}\, f_i^{n/A}(x,Q)$$

(Schienbein et. al. arXiv:0907.2357v2)

- Hessian error sets for the nPDFs are provided for the parameters of the nuclear correction.

nCTEQ Errors vs CT10 Errors

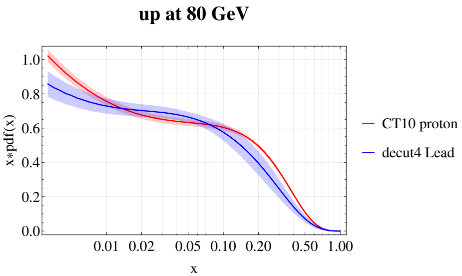

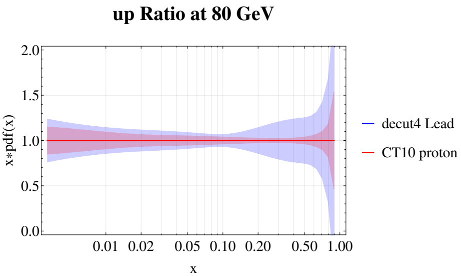

- Error sets have been created for the nCTEQ PDFs by A. Kusina, K. Kovařík, and T. Ježo.
- The error sets are over 16 eigenvectors. Each family contains 34 PDF sets.

ATLAS measurement

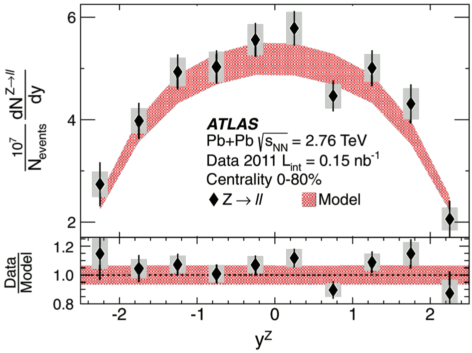

(ATLAS Collaboration, PRL 110,022301 92013))

- In January of 2013, ATLAS released the results of their Z boson rapidity distribution for PbPb collisions at $2.76\mathrm{TeV}$.
- ATLAS observed 1995 candidate events corresponding to $0.15\mathrm{nb}^{-1}$ of integrated Luminosity.

ATLAS measurement

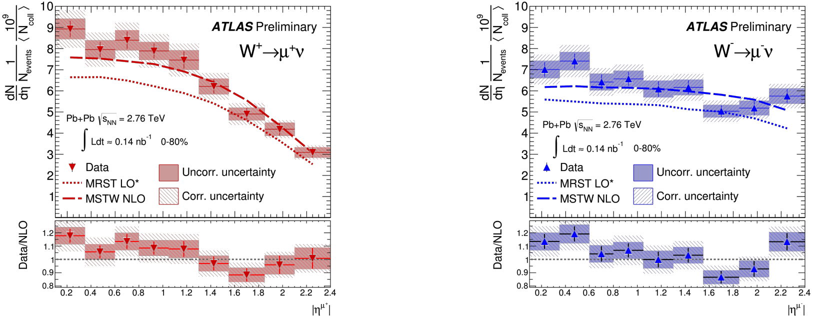

(ATLAS Collaboration, ATLAS-CONF-2013-106)

- In November of 2013, ATLAS released the result of their μ^+ and μ^- rapidity measurements in PbPb.
- All of the heavy ion runs have been compared to predictions made with NLO PDFs.

CMS measurement

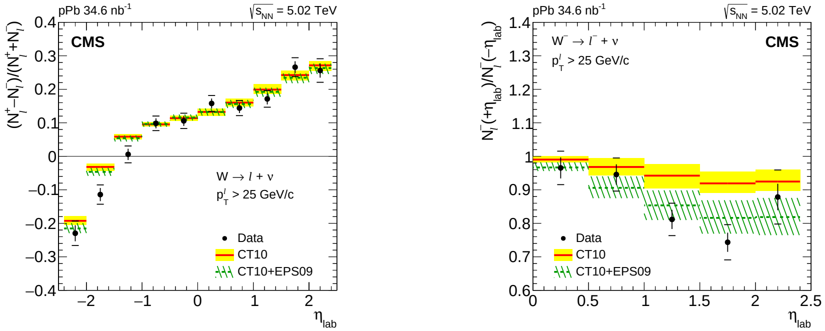

(CMS Collaboration, CMS-HIN-13-007, CERN-PH-EP-2015-054)

- In March of 2015, CMS released the result of their μ^+ and μ^- rapidity measurements in pPb collisions at $5.02\mathrm{TeV}$.
- LHC experiments have yet to detect any nuclear modifications to Vector Boson cross sections.

Heavy Ion Collisions

Vector Boson Production

- High Energy collisions at the LHC are capable of producing many electroweak bosons (W/Z) at high absolute rapidity.
- Properties of these bosons are well constrained making them ideal "standard candle" measurements for detector calibration.
- The hadronic cross section for Drell-Yan pair production is written

$$\frac{d\sigma}{dQ^2\,dy} = \sum_{a,b} \int_0^1 d\xi_1 \int_0^1 d\xi_2 \frac{d\hat{\sigma}}{dQ^2 dy} f_{a/A}(\xi_1) f_{b/B}(\xi_2)$$

- At LO we can make the approximation,

$$\xi_1 \approx x_1 \equiv \tau e^{y}, \qquad \xi_2 \approx x_2 \equiv \tau e^{-y},$$

where

$$\tau \equiv \frac{Q}{\sqrt{S}}.$$

Vector Boson Production

- This means that rapidity measurements for on-shell vector boson production provide a method for probing the x dependence of the PDFs.

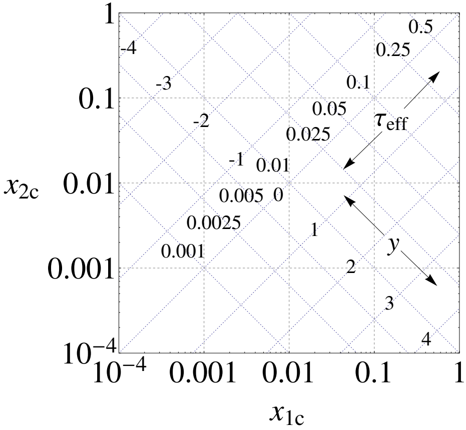

$$\tau \equiv \frac{Q}{\sqrt{S}}.$$

(Guzey,V. et al, arXiv:1212.5344v1)

PDF Contributions

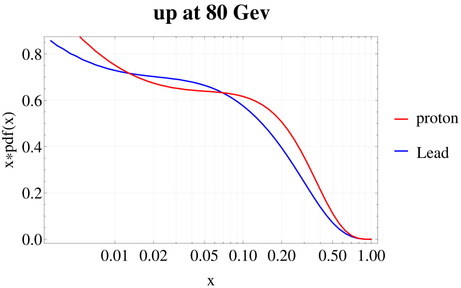

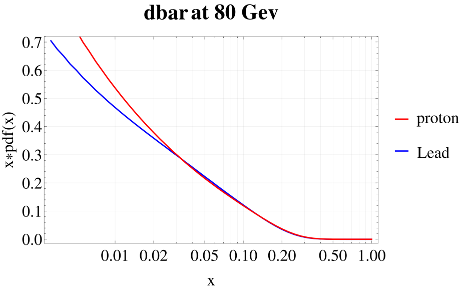

- For $W^{\pm}\,(Z)$ production at 2.76TeV, $\tau \approx 0.029\,(0.033)$
- For $W^{\pm}\,(Z)$ production at 5.02TeV, $\tau \approx 0.016\,(0.018)$

Results

PbPb vs. p-p Rapidity

- There is an observable shape change for on-shell W^+ production. The difference is up to 20 % in some regions of parameter space.

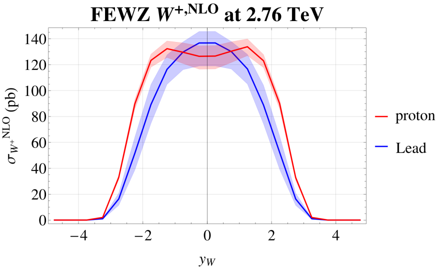

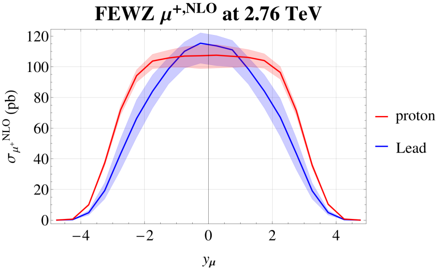

- These differences should be seen with a higher integrated luminosity for PbPb collisions.

PbPb vs. p-p Rapidity

- There is an observable shape change for on-shell W^+ production. The difference is up to 20 % in some regions of parameter space.

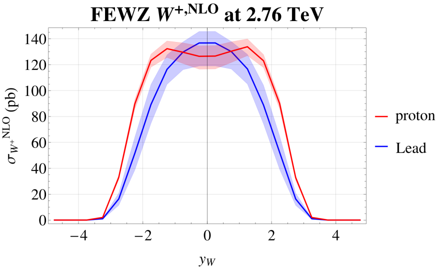

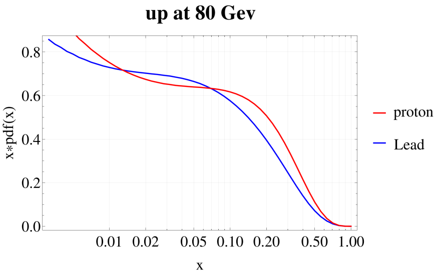

- These differences should be seen with a higher integrated luminosity for PbPb collisions.

PDF Correlations

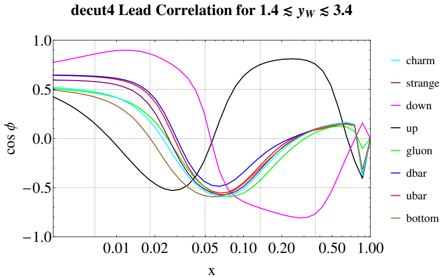

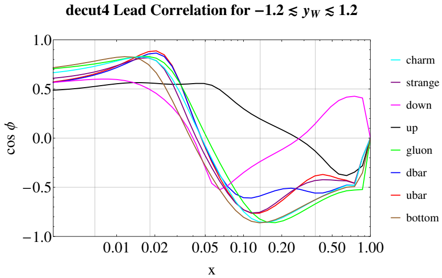

- In the high absolute rapidity region, the error is dominated by the uncertainty on the down PDF.
- The up and down distributions are anti-correlated in x allowing for flavor decomposition.
- In the central region, the $\bar{u}$ and $\bar{d}$ uncertainty provides the largest contribution

pPb Rapidity

- The shape of the pPb cross sections can be predicted by looking at the nuclear corrections to the PDFs.

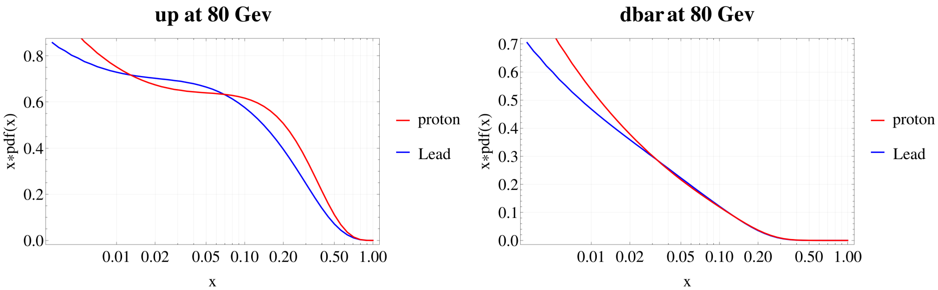

- These predictions are presented in the Center of Momentum frame of the two nuclei. The experimental results include a 0.465 rapidity shift.

PDF Contributions

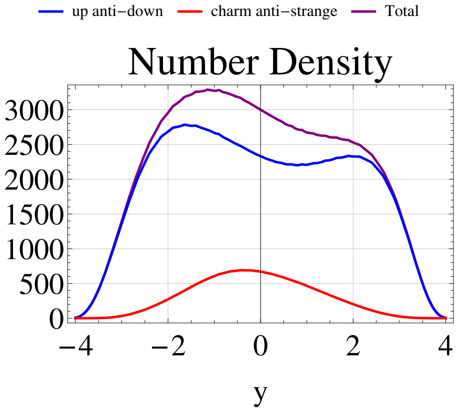

- Here we look at the $u - \bar{d}$ and $c - \bar{s}$ interactions for W^+ production.

$$\sigma_{DY} \sim f_{a/A}(\tau e^{y}, Q) * f_{b/B}(\tau e^{-y}, Q)$$

pPb W Rapidity

- The resulting W^+ predictions with nCTEQ15 show significant differences to the predictions using EPS09 nuclear corrections.

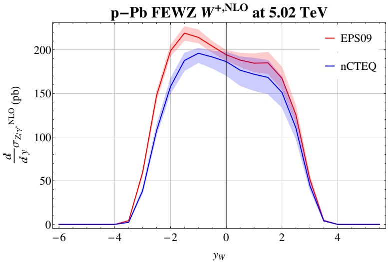

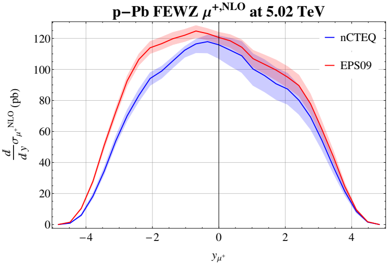

- Current CMS measurements show tension with the EPS09 predictions. A direct comparison to CMS data is underway to see if better agreement is possible with nCTEQ PDFs.

pPb W Rapidity

- The resulting W^- predictions with nCTEQ15 also show differences to the predictions using EPS09 nuclear corrections.

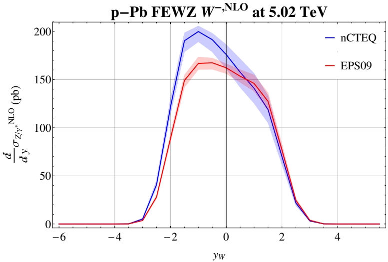

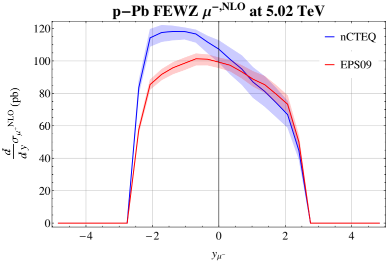

- Differences with EPS09 are visable for all Vector Bosons and for the resulting muon distributions.

Conclusions and Future Work

- Nuclear modifications to PbPb cross sections are up to 20% and should be visible with a higher integrated luminosity.
- Work is underway to produce predictions at $8.16\mathrm{TeV}$ and $8.80\mathrm{TeV}$ for pPb cross sections.
- A comparison to AMC@NLO is in progress. AMC will be used in the next nCTEQ fit containing LHC data.
- Current results from CMS show tension with EPS09 predictions. A comparison of nCTEQ predictions to recent CMS results is underway.
- The nCTEQ predictions show significant differences to the EPS predictions at high negative rapidity where the ratio $d(x, Q_0)/u(x, Q_0)$ is important.

nCTEQ Collaboration

- A. Kusina
  - Email: kusina@lpsc.in2p3.fr
- K. Kovařík
  - Email: karol.kovarik@uni-muenster.de
- T. Ježo
  - Email: tomas.jezo@mib.infn.it
- D. B. Clark
  - Email: dbclark@smu.edu
- C. Keppel
  - Email: keppel@jlab.org
- F. Lyonnet
  - Email: flyonnet@smu.edu
- J.G. Morfín
  - Email: morfin@fnal.gov
- F. I. Olness (Advisor)
  - Email: olness@smu.edu
- J.F. Owens
  - Email: owens@hep.fsu.edu
- I. Schienbein
  - Email: ingo.schienbein@lpsc.in2p3.fr
- J. Y. Yu
  - Email: yu@physics.smu.edu

Backup Slides

PDFs and Fitting

Scattering

- Scattering gives us a tool to study the inner structure of nuclei.
- All scattering is a direct decedent of Rutherford's scattering.

$$\left(\frac{d\sigma}{d\Omega}\right)_{Rutherford} = \frac{(\alpha Z)^2}{4E^2 \sin^4 \frac{\theta}{2}}$$

Elastic Scattering

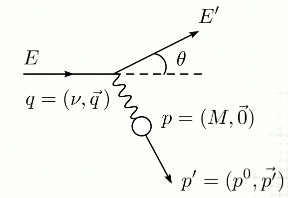

- Information on the structure of the atom can be determined from the energy and the scattering angle of the probe.

DIS

- Scattering off of extended objects introduces structure functions.
- These functions describe non-perturbative physics and contain new kinematic variables.

DIS

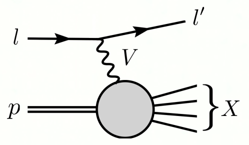

$$l\,(k) + p\,(p) \to l'\,(k') + X$$

Kinematics

$$q = k - k'$$

$$Q^2 = -q^2$$

$$x = \frac{Q^2}{2p\dot{q}}$$

DIS

- The cross section for DIS is written in terms of the structure functions
$$\frac{d\sigma}{dE' d\Omega} = \frac{\alpha^2}{4E^2 \sin^4 \frac{\theta}{2}} \left(\frac{2F_1(x, Q^2)}{M} \sin^2 \frac{\theta}{2} + \frac{F_2(x, Q^2)}{E - E'} \cos^2 \frac{\theta}{2} \right)$$
- We can write the cross section for inelastic scattering as an incoherent sum of elastic scatterings off constituents of the proton. This is the parton model.

$$\frac{d\sigma}{dx\, dQ^2} = \sum_q \int d\xi \; f_q(\xi) \left(\frac{d\hat{\sigma}^{eq}}{dx\, dQ^2} \right)$$

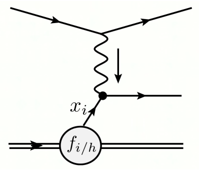

PDFs

- Structure function at LO

$$F_2(x) = \sum_q e_q^2 \int d\xi \; x \; f_q(\xi)\delta\left(\xi - \frac{Q^2}{2p\dot{q}}\right)$$

- The PDFs are number densities at LO

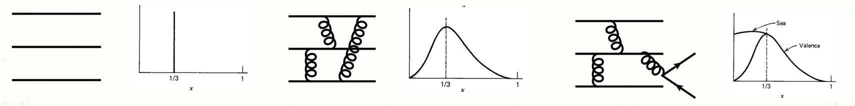

Free Quarks   Bound Quarks   Bound + QCD Effects

Scale Dependence of PDFs

- The scale dependence of the PDFs is introduced through the DGLAP equations

$$\frac{df_q(x,Q^2)}{d\log Q^2} = \frac{\alpha_s(Q^2)}{2\pi}\int_x^1 \frac{d\xi}{xi}\left[P_{qq}\left(\frac{x}{\xi}\right) f_q(\xi,Q^2) + P_{qg}\left(\frac{x}{\xi}\right) f_g(\xi,Q^2)\right]$$

$$\frac{df_g(x,Q^2)}{d\log Q^2} = \frac{\alpha_s(Q^2)}{2\pi}\int_x^1 \frac{d\xi}{xi}\left[P_{gg}\left(\frac{x}{\xi}\right) f_g(\xi,Q^2) + P_{gq}\left(\frac{x}{\xi}\right) f_q(\xi,Q^2)\right]$$

- QCD factorization proves the universality of the splitting functions an allows for separation of hadronic processes into perturbative and non-perturbative parts.

Fitting of PDFs

- To fit the PDFs:
  - First, we decouple the splitting functions by rotating into a new basis.
  - Next, we fit the PDFs to data at some initial scale Q_0^2.
  - Finally, we evolve the PDFs using the DGLAP equations.

- The universality of the PDFs then allows us to use them for any hadronic process.
  E.g. Drell-Yan di-lepton production at the LHC

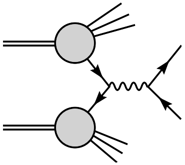

$$\sigma = \sum_{a,b} \int dx_1\, dx_2\, f_{a/h_1}(x_1, Q^2)\, f_{b/h_2}(x_2, Q^2)\, \sigma_{a\hat{b}\to X}(x_1 x_2 s)$$

Fitting of PDFs

- Every PDF fit begins with a parameterization of ~ 30 free parameters.
- The x dependence is neither predicted or constrained by pQCD.
- The parameterization should be loose enough that it eliminates bias from the PDF fit. In practice this is not (completely) possible.
- A generic PDF parameterization is given by

$$xf_k(x, Q_0) = c_0 x^{c_1}(1-x)^{c_2} P_k(x)$$

  where k is the parton being fit and $P_k(x)$ is a polynomial function of Bjorken-x.
- A best χ^2 fit to data (mostly DIS and DY) is then produced.

- Experimental data is chosen to provide coverage in x and Q^2 plane.

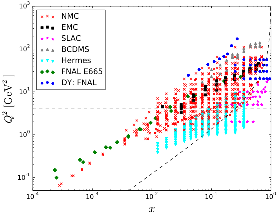

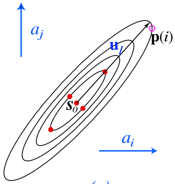

(a)
Original parameter basis

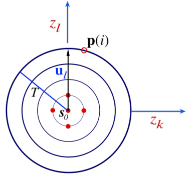

(b)
Orthonormal eigenvector basis

- Errors are typically provided by diagonalizing the Hessian

$$\chi^2(a) = \chi_0^2 + \frac{1}{2}\frac{\partial\chi^2}{\partial a_i \partial a_j}(a - a_0)_i(a - a_0)_j + \ldots \rightarrow \chi_0^2 + \sum iz_i^2$$

Fitting PDFs

- The PDFs are further constrained by imposing the number and momentum sum rules.
- For the proton:

$$\int_0^1 dx\,[u(x) - \bar{u}(x)] = 2$$

$$\int_0^1 dx\,\left[d(x) - \bar{d}(x)\right] = 1$$

$$\sum_i \int_0^1 dx\, x f_i(x) = 1$$

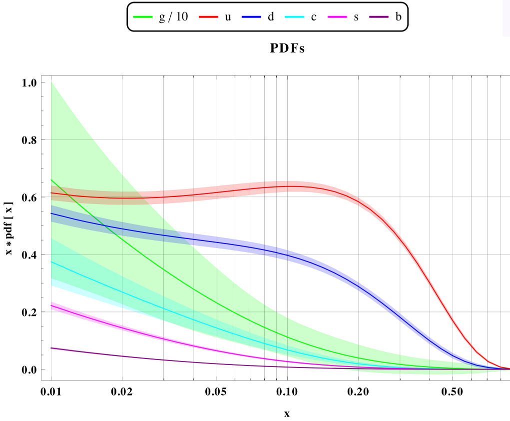

CTEQ 10

LO Rapidity Calculation

- A LO calculation of rapidity shows shape changes due to the softening of the $u\,(x, Q)$ and $\bar{d}\,(x, Q)$ PDFs.

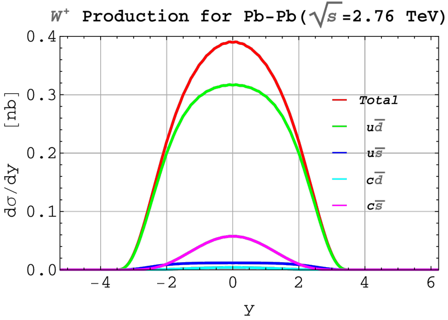

PbPb

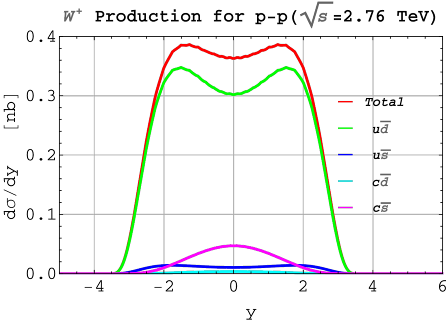

p-p

PDF Comparison

- The nCTEQ proton PDF set gives similar predictions to other commonly used sets.

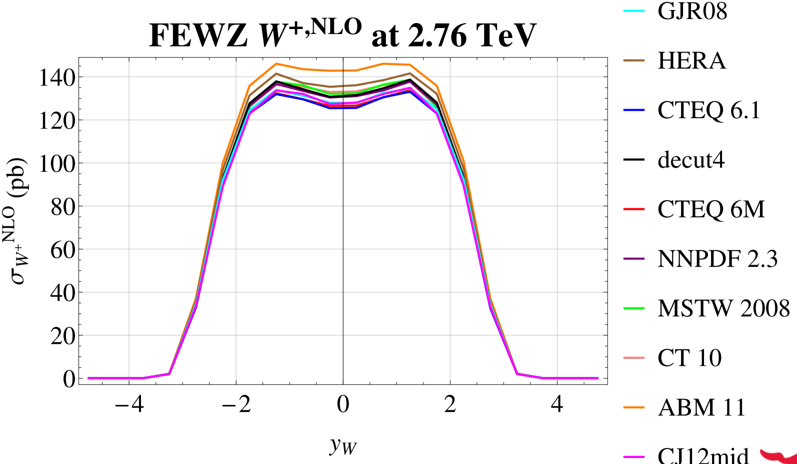

PbPb vs. pp rapidity

- No shape change for on-shell Z and W^- rapidity is found as we move from the proton PDFs to Lead.

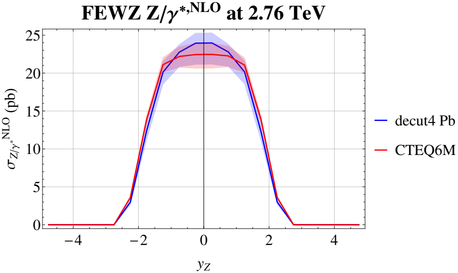

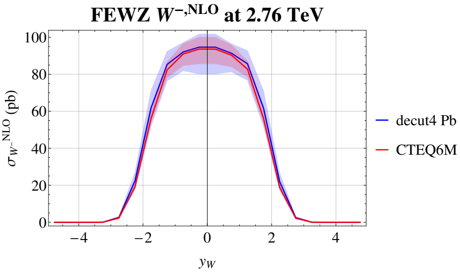

- The shapes of the lepton distributions for these bosons are also indistinguishable.